Investigation of cathode properties of two-dimensional NbS_2Cl_2 for Li and Na-ion batteries using density functional theory

To cite this article: Arul Raj Natarajan *et al* 2024 *Electron. Struct.* **6** 025004

IOP Publishing Electron. Struct. 6 (2024) 025004 https://doi.org/10.1088/2516-1075/ad46b5

Electronic Structure

PAPER

Investigation of cathode properties of two-dimensional NbS_2Cl_2 for Li and Na-ion batteries using density functional theory

Arul Raj Natarajan[1], **Bhalchandra S Pujari**[2], **G Vaitheeswaran**[3] and **V Kanchana**[1,*]

[1] Department of Physics, Indian Institute of Technology Hyderabad, Kandi, 502285 Sangareddy, Telangana, India
[2] Department of Scientific Computing, Modeling and Simulation, Savitribai Phule Pune University, Ganeshkind, Pune 411007, Maharashtra, India
[3] School of Physics, University of Hyderabad, Prof. C. R. Rao Road, Gachibowli, Hyderabad 500046, Telangana, India
[*] Author to whom any correspondence should be addressed.

E-mail: kanchana@phy.iith.ac.in

Keywords: two-dimensional materials, cathode, diffusion barrier, thermodynamic properties

RECEIVED
13 December 2023

ACCEPTED FOR PUBLICATION
2 May 2024

PUBLISHED
24 May 2024

Abstract

Exploring novel two-dimensional materials (2D) for electrode and electrochemical storage applications stands as a pivotal pursuit in advancing renewable energy technologies. While recent research has predominantly focused on anode materials, cathode materials have received comparatively lesser attention. This study delves into the potential cathode applications of the novel two-dimensional material NbS_2Cl_2 using density functional theory. Fundamental properties, encompassing electronic and thermodynamic attributes, were scrutinized to comprehend the material's characteristics. Our investigation extended to examining the adsorption and diffusion properties of these electrode materials. Comprehensive calculations of mechanical and thermodynamic properties reaffirmed the stability of this system. Upon adsorption of Li/Na atoms, the conducting nature emerged, evident through charge density difference and projected density of states. Our findings notably reveal minimal diffusion barriers of 1.5 eV and 0.35 eV for Li and Na atoms. Moreover, the observed open circuit voltages for adsorbed Li and Na ions were 4.69 V and 2.62 V, respectively. The calculated theoretical capacity for adsorbed Li-ion on 2D-NbS_2Cl_2 is 400 mAh g^{-1}, while for Na-ion adsorption, it is 353 mAh g^{-1}, awaiting validation through future experimental verifications.

1. Introduction

Rapidly changing climate conditions with catastrophic effects on our ecology due to global warming have been worsened by the continual use of fossil fuels for our energy requirements [1–4]. Increasing population and industrial growth demand more energy, and decreasing fossil fuels and growing environmental problems need to search for renewable energy resources. Energy resources like solar and wind have reached a developed stage and are used everywhere. It remains a significant problem to securely and smoothly integrate these renewable but inconsistent resources into electricity supply systems [3, 5]. Batteries play a massive role in this regard, significantly impacting consumer electronics and electric automotive industries [6–8]. Therefore, a lot of effort has been put together by the global scientific community to explore novel battery materials with high energy density, longer life span, safety and low cost [9–11].

Due to their significant surface-to-volume ratio and tunable band gap, two-dimensional (2D) materials are highly suitable for electrode properties [12, 13]. 2D materials can improve electrochemical characteristics by increasing electrical conductivity [14]. They have potentially low diffusion barriers which could lead to high cycling rates [15]. 2D materials have significant potential for thermal management applications due to their intrinsic heat conductivity [16]. Though several well-known 2D materials such as graphene [17, 18], chalcogenides [19, 20], metal oxides [21] and MXenes [22, 23] have been studied extensively, the challenge associated with electrodes and electrolytes still persists. Therefore, it is imperative among the energy storage community to look for potential new candidates as battery materials.

Today, many essential characteristics of lithium-ion batteries can be precisely predicted by density functional theory (DFT) due to the enormous advancements made in computational approaches over the last two decades. With the ability to compare experimental data quantitatively and provide insight into basic processes, including ionic diffusion mechanisms and electronic structure effects, computational tools have become indispensable in battery-related research [24]. Monolayer NbS_2Cl_2 has attracted researchers recently due to its multiple applications, such as thermoelectric, optical and water splitting [25]. So, in this paper, we studied the electrode properties of monolayer NbS_2Cl_2 using DFT.

The study is structured as follows: section 2 presents the computational methods, section 3 presents the results and discussions, and section 4 concludes the work.

2. Computational details

The study employed the Vienna *ab initio* simulation package (VASP) with the DFT approach for both structural optimization and investigation of electronic properties [26]. A plane wave energy cut-off of 600 eV was chosen, and the Perdew–Burke–Ernzerhof variant of the generalized gradient approximation was applied for exchange–correlation potential [27]. To ensure convergence in energy and forces during structural optimization, tolerance limits of 10^{-6} eV and 0.01 eV $Å^{-1}$, respectively, were set. Considering the weak interactions between layers, van der Waals corrections (DFT-D3) as proposed by Grimme were included in the calculations [28]. To prevent periodic interactions between two layers, a vacuum space of 20 Å was introduced in the c-direction. A $2 \times 2 \times 1$ supercell was utilized to relax the structure and examine the electronic properties related to the adsorption of Li/Na on the surface of the NbS_2Cl_2 monolayer. All calculations employed a Γ-centred Monkhorst–Pack $12 \times 6 \times 1$ *k*-grid to represent the Brillouin zone [29]. Thermal stability properties were investigated using the PHONOPY code [30–32]. The diffusion barriers of ions were computed using the Climbing Image of the Nudged Elastic Band (CI-NEB) approach, with 12 intermediate images between fully optimized initial and final structures using Quantum-ATK [33–35].

3. Results and discussions

3.1. Structural and electronic properties

NbS_2Cl_2 has a monoclinic crystal structure with a $C2/m$ space group. The unit-cell contains 4 Niobium, 8 Sulphur, and 8 Chlorine atoms. The optimized $2 \times 2 \times 2$ supercell of bulk structure is shown in figure 1(a). In the NbS_2Cl_2 monolayer, Nb atoms appear in pairs. Each Nb–Nb pair is connected to four S atoms to create a cage-like Nb_2S_4 unit. The bond length between Nb–Nb (2.87 Å) is longer than that between S–S (1.99 Å). The bond lengths between Nb–S (2.48 Å) and Nb–Cl (2.59 Å) are nearly the same. These values are consistent with the experimentally reported values [36]. In bulk, the layers are stacked along the 'c' axis and held together by weak van der Waals interactions between interlayer atoms. Therefore, we cleaved a single layer from the stacking of bulk along the 'c' axis to form a monolayer and adsorped the Li/Na atom as shown in figures 1(b) and (c). Next, we calculated the cohesive energy to investigate the stability of the system and the equation given below [37],

$$E_{\text{coh}} = \frac{m_1 \times E(Nb) + m_2 \times E(S) + m_3 \times E(Cl) + m_4 \times E(x) - E(xNbS_2Cl_2)}{m_1 + m_2 + m_3 + m_4} \tag{1}$$

where x = Li/Na and E(xNbS$_2$Cl$_2$), E(Nb), E(S), E(Cl) and E(x) are energies of x adsorped in NbS_2Cl_2, isolated Nb, S, Cl and x respectively. m_1, m_2, m_3 and m_4 are number of Nb, S, Cl and x in the supercell. We have investigated the cohesive energy of NbS_2Cl_2 after adsorping Li and Na which are −1.68 eV and −2.40 eV. The negative value indicates stability of the system.

We have calculated the charge density difference($\Delta\rho$) to study the charge transfer between layer and metal atom. The $\Delta\rho$ is defined as,

$$\Delta\rho = \rho_{xNbS_2Cl_2} - \rho_{NbS_2Cl_2} - \rho_x \tag{2}$$

where $\rho_{xNbS_2Cl_2}$, $\rho_{NbS_2Cl_2}$ and ρ_x are charge density of x(Li/Na) adsorped and pristine layer of NbS_2Cl_2 and single metal atom, respectively. The calculated $\Delta\rho$ for studied compound is shown in figure 2. The cyan-coloured area shows a depletion in charge density, while the yellow-coloured region indicates an accumulation in charge density. We observed a significant charge transfer between adsorped metal atoms to monolayer NbS_2Cl_2. Figure 3 displays the projected density of states or NbS_2Cl_2, $LiNbS_2Cl_2$, and $NaNbS_2Cl_2$. The structure of pristine NbS_2Cl_2 is semiconductor in nature. The Nb-d state contributes more to the valence band than the S-p and Cl-p states. S-p orbitals contribute more than Nb-d and Cl-p orbitals in the conduction band at the Fermi level. After adsorping Li and Na ions, it becomes metallic which is an

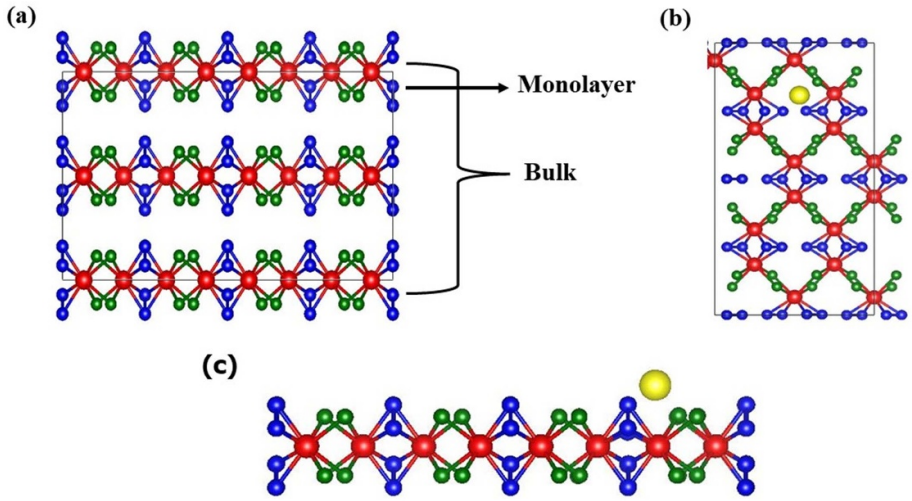

Figure 1. (a) Bulk structure in 2 × 2 × 2 supercell and (b), (c) side and top view of the monolayer in 2 × 2 × 1 supercell with adsorped Na atom. The atoms of Nb, S, Cl, and Li/Na are represented by the colours red, blue, green, and yellow.

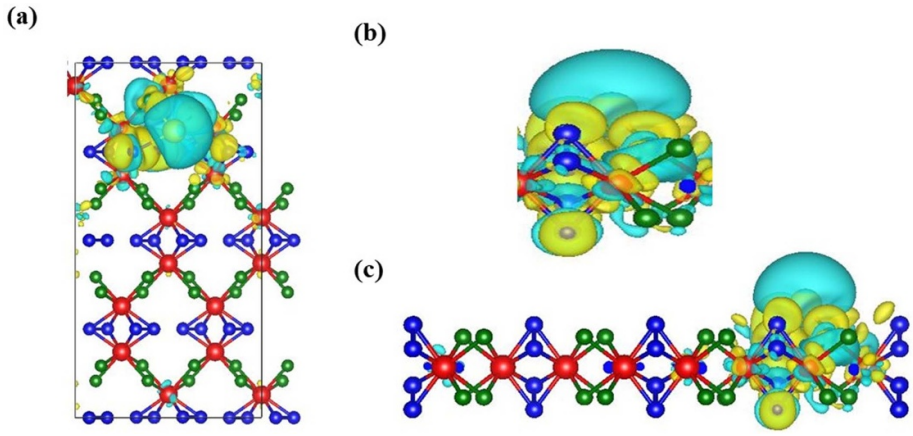

Figure 2. (a), (c) Side and top view of the charge density difference and (b) charge density cloud around the Na-atom.

important property for battery materials [38, 39]. This metallic transition is mainly due to the contribution of unpaired electrons in Li/Na to the Fermi level. During the process of charging and discharging, it is observed that the mechanical properties of the cathode materials undergo notable alterations, resulting in substantial deformation. This deformation, in turn, can give rise to the fracturing of the electrode. The structural distortion of the cathode material induces significant deterioration, manifesting as increased capacity decay and compromised cycling longevity. Elastic constants are crucial in assessing the material's mechanical stability [40]. The evaluated diagonal component within the elastic constants C_{11} and C_{22} manifests as 72 and 100 GPa, respectively, thereby corroborating the inherent stability of the system. The observed elastic constants of an investigated compound are nearly equal to other reported two-dimensional materials of the monoclinic structure [41, 42].

3.2. Thermodynamic properties

Phonon dispersion calculation was performed to validate thermodynamic stability of the system which is shown in figure 4(a). The absence of imaginary phonon modes in the calculated phonon dispersion reveals the investigated system is dynamically stable. Within the quasi-harmonic approximation, the integration over the phonon density of states is performed to calculate the temperature-dependent specific heat capacity (C_v), Helmholtz free energy (F) and entropy (S) using the following expression [43],

$$C_v = 3nNK_B \int_0^{\omega_{max}} \left(\frac{h\omega}{2\kappa_B T}\right)^2 csch^2\left(\frac{h\omega}{2\kappa_B T}\right) g(\omega)\, d\omega \quad (3)$$

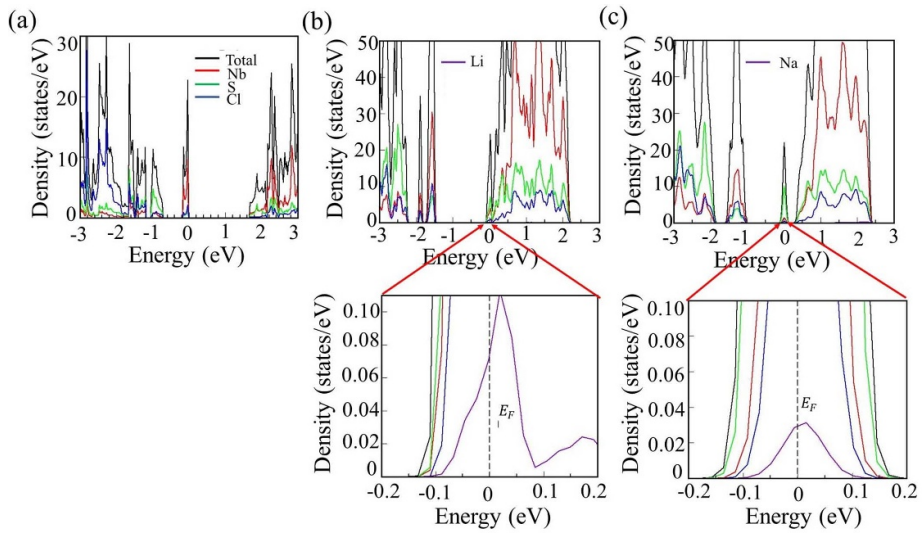

Figure 3. The partial density of states for (a) pristine structure (b), (c) after adsorping Li/Na atom in the monolayer.

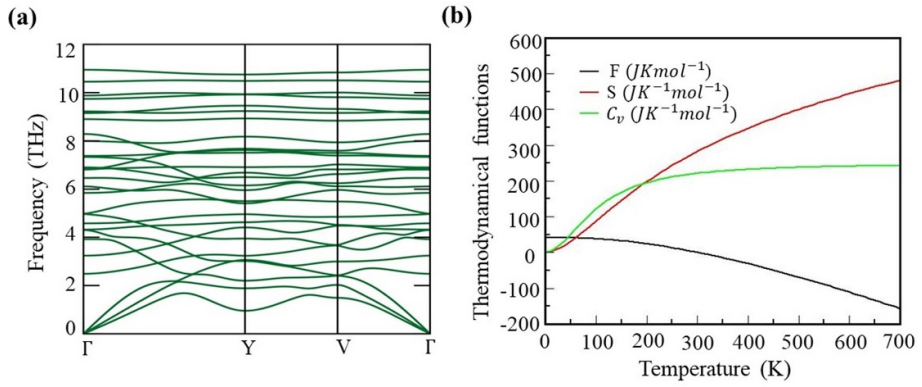

Figure 4. (a) Phonon dispersion and (b) thermodynamic coefficients of the monolayer NbS_2Cl_2.

$$F = 3nNK_B T \int_0^{\omega_{max}} \ln\left(2\sinh\left(\frac{h\omega}{2\kappa_B T}\right)\right) g(\omega)\, d\omega \tag{4}$$

$$S = 3nNK_B \int_0^{\omega_{max}} \left[\left(\frac{h\omega}{2\kappa_B T}\right)\coth\left(\frac{h\omega}{2\kappa_B T}\right) - \ln\left(2\sinh\left(\frac{h\omega}{2\kappa_B T}\right)\right)\right] g(\omega)\, d\omega \tag{5}$$

where κ_B is the Boltzmann constant, Ω_{max} is the largest phonon frequency, n is the number of atoms per unit cell, N is the number of unit cells. Figure 4(b) displays the thermodynamic properties of NbS_2Cl_2. The Helmholtz free energy decreases as the temperature increases and reaches -155.46 J K mol^{-1} at 700 K. As a function of temperature, the free energy is discovered to decrease progressively and become negative. As the temperature increases from 0 to 300 K, the constant volume-specific heat capacities (C_v) rise significantly, reaching approximately 220 J K^{-1} mol^{-1} and it approaches the classical asymptotic limit of Dulong–Petit law. Due to thermal agitation, the system's entropy (S) increases with respect to temperature [44]. The entropy (S) increases significantly from 0 to 285 J K^{-1} mol^{-1} at 300 K.

3.3. Diffusion properties

One of the most crucial factors in determining whether an electrode material is suitable for use with rechargeable batteries is the mobility of the adsorping ion, which determines the charge–discharge rate of rechargeable batteries [45, 46]. Desirable qualities for an effective electrode material include high mobility within the layer and minimal diffusion barriers [47]. We have calculated different possible pathways for the diffusion of Li/Na and their corresponding energy barriers, which are shown in figures 5 and 6. We observed that there are two possible paths for ion mobility. The first path (path-I) is between x_1 and x_2, whereas the

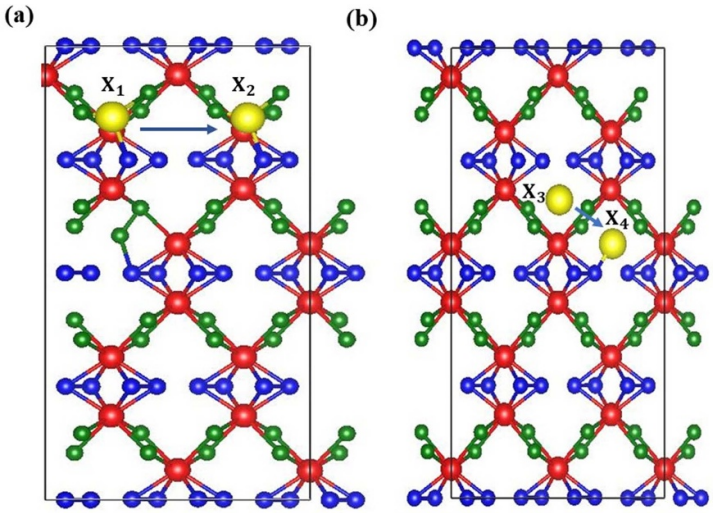

Figure 5. (a) Path-I and (b) path-II for the nudged elastic band.

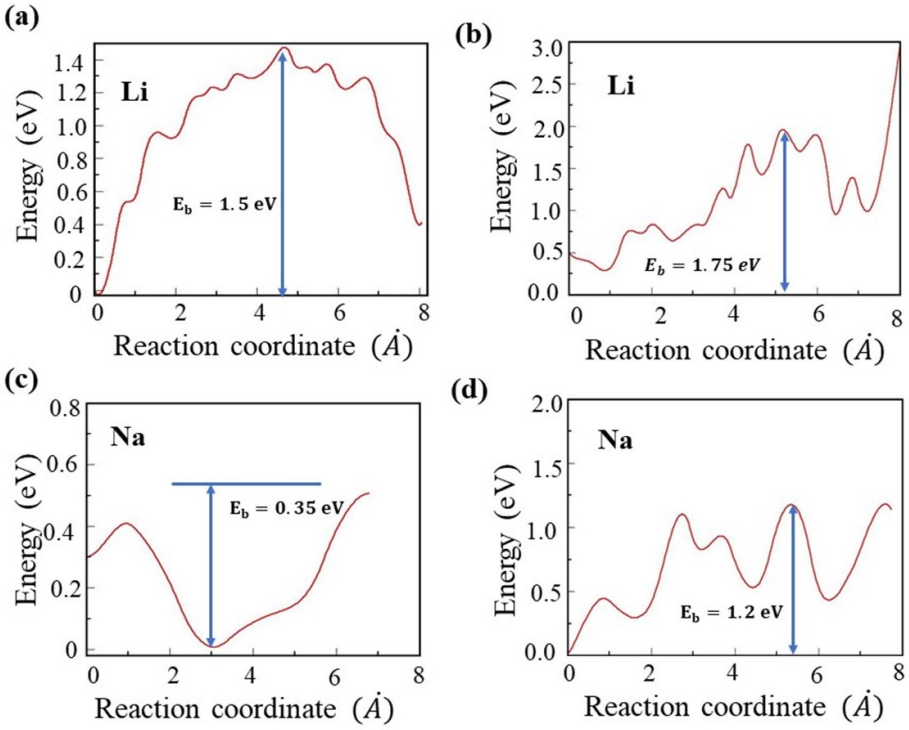

Figure 6. (a), (c) Energy barrier for the path-I and (b), (d) energy barrier for path-II.

second path (path-II) is between x_3 and x_4. Li and Na ions in path-I have an activation energy of 1.5 eV and 0.35 eV, respectively, whereas path-II has an activation energy of 1.75 eV and 1.2 eV, respectively. It shows that the energy of the diffusion barrier decreases with increasing ionic radius [48]. Among the two possible paths, path-1 has the minimum activation energy compared to path-2 due to less interaction with the structure. The calculated barrier energies are very low value compared to earlier reported values such as MoS_2(0.6 eV) [49], SiC_7(0.8 eV) [39] and $VOPO_4$(0.62 eV) [50].

3.4. Theoretical capacity and open circuit voltage (OCV)

The storage capacity is a crucial factor in determining the effective electrode properties. The theoretical capacity, C , was given by

$$C = \frac{nzF}{M_f}. \tag{6}$$

Here, n and z represent the number and charge of adsorped Li/Na ions in the pristine structure. M_f and F are molecular weight and Faraday constant, respectively. We discovered that the theoretical capacity of Li and Na ions is 400 mAh g^{-1} and 353 mAh g^{-1}, respectively, which is greater than that of MoS_2 (146 mAh g^{-1}) [49], Mo_2C (132 mAh g^{-1}) [38] and boron phosphide (143 mAh g^{-1}) [51]. Calculating the OCV is an essential parameter of electrode material. If x is the number of adsorbed adatoms on NbS_2Cl_2, the OCV can be calculated as, [52]

$$OCV = \frac{\Delta G_f}{x} \approx \frac{-E_{\text{ad}}}{x} \tag{7}$$

where E_{ad} is adsorption energy of the investigated compound which is $E_{ad} = E_{NaNbS_2Cl_2} - E_{NbS_2Cl_2} - E_{Na}$. The calculated OCVs for Li and Na are 4.69 V and 2.62 V, respectively which is higher than other state-of-art investigated cathode materials such as $LiNbS_2O_2$ (4.2 V) [53] and $LiCoO_2$ (4.5 V) [54]. Our investigated compound can be suitable for potential cathode material.

4. Conclusion

This study employs DFT to investigate the thermodynamic and electrode characteristics of monolayer NbS_2Cl_2. Our findings reveal that upon binding Li/Na to the monolayer's surface, the computed density of states showcases a metallic nature an essential property for rechargeable battery materials. The phonon spectra and elastic constants affirm the compound's robust thermal and mechanical stability. Notably, our research identifies remarkably low diffusion barriers of 1.5 eV and 0.35 eV for Li and Na atoms, indicating highly efficient diffusion mobility. Moreover, our investigation highlights superior charge/discharge rates for Na-ion batteries compared to Li-ion batteries. We determine a Li-ion capacity of 400 mAh g^{-1}, hinting at potential avenues for future enhancements.

Data availability statement

The data cannot be made publicly available upon publication because they are not available in a format that is sufficiently accessible or reusable by other researchers. The data that support the findings of this study are available upon reasonable request from the authors.

Acknowledgments

The authors A R N, and V K would like to thank IIT Hyderabad for computational facility. A R N would like to thank CSIR for fellowship. A R N and V K would like to acknowledge National Supercomputing Mission (NSM) for providing computing resources of 'PARAM SEVA' at IIT, Hyderabad, which is implemented by C-DAC and supported by the Ministry of Electronics and Information Technology (MeitY) and Department of Science and Technology (DST), Government of India. G V acknowledges, CMSD, University of Hyderabad for providing computational facility.

ORCID iDs

Arul Raj Natarajan https://orcid.org/0009-0002-9579-7747
Bhalchandra S Pujari https://orcid.org/0000-0002-5828-3766
G Vaitheeswaran https://orcid.org/0000-0002-2320-7667
V Kanchana https://orcid.org/0000-0003-1575-9936

References

[1] Tarascon J M and Armand M 2001 *Nature* **414** 359–67
[2] Rockström J, Gaffney O, Rogelj J, Meinshausen M, Nakicenovic N and Schellnhuber H J 2017 *Science* **355** 1269–71
[3] Jacobson M Z and Delucchi M A 2011 *Energy Policy* **39** 1154–69
[4] Bhatt M D and O'Dwyer C 2015 *Phys. Chem. Chem. Phys.* **17** 4799–844
[5] Deng Q, Fu Y, Zhu C and Yu Y 2019 *Small* **15** 1804884
[6] Cano Z P, Banham D, Ye S, Hintennach A, Lu J, Fowler M and Chen Z 2018 *Nat. Energy* **3** 279–89
[7] Bruce P G, Freunberger S A, Hardwick L J and Tarascon J M 2012 *Nat. Mater.* **11** 19–29
[8] Goodenough J B and Park K S 2013 *J. Am. Chem. Soc.* **135** 1167–76
[9] Zubi G, Dufo-López R, Carvalho M and Pasaoglu G 2018 *Renew. Sustain. Energy Rev.* **89** 292–308
[10] Kim T, Song W, Son D Y, Ono L K and Qi Y 2019 *J. Mater. Chem. A* **7** 2942–64
[11] Vaalma C, Buchholz D, Weil M and Passerini S 2018 *Nat. Rev. Mater.* **3** 1–11
[12] Peng L, Zhu Y, Chen D, Ruoff R S and Yu G 2016 *Adv. Energy Mater.* **6** 1600025
[13] Pomerantseva E and Gogotsi Y 2017 *Nat. Energy* **2** 1–6

[14] Shi L and Zhao T 2017 *J. Mater. Chem.* A **5** 3735–58
[15] Chowdhury C and Datta A 2017 *J. Phys. Chem. Lett.* **8** 2909–16
[16] Song H, Liu J, Liu B, Wu J, Cheng H M and Kang F 2018 *Joule* **2** 442–63
[17] Lee J K, Smith K B, Hayner C M and Kung H H 2010 *Chem. Commun.* **46** 2025–7
[18] Yoo E, Kim J, Hosono E, Zhou H s, Kudo T and Honma I 2008 *Nano Lett.* **8** 2277–82
[19] Huang J, Wei Z, Liao J, Ni W, Wang C and Ma J 2019 *J. Energy Chem.* **33** 100–24
[20] Li Y *et al* 2018 *Adv. Energy Mater.* **8** 1800927
[21] Shen L, Dong Q, Zhu G, Dai Z, Zhang Y, Wang W and Dong X 2018 *Adv. Mater. Interfaces* **5** 1800362
[22] Er D, Li J, Naguib M, Gogotsi Y and Shenoy V B 2014 *ACS Appl. Mater. Interfaces* **6** 11173–9
[23] Ladha D G 2019 *Mater. Today Chem.* **11** 94–111
[24] Urban A, Seo D H and Ceder G 2016 *npj Comput. Mater.* **2** 1–13
[25] Qiao M, Wang C, Jing Y, Zhou X and Li Y 2021 *FlatChem* **27** 100237
[26] Kresse G and Joubert D 1999 *Phys. Rev.* B **59** 1758
[27] Perdew J P, Burke K and Ernzerhof M 1996 *Phys. Rev. Lett.* **77** 3865
[28] Grimme S, Antony J, Ehrlich S and Krieg H 2010 *J. Chem. Phys.* **132** 154104
[29] Monkhorst H J and Pack J D 1976 *Phys. Rev.* B **13** 5188
[30] Togo A and Tanaka I 2015 *Scr. Mater.* **108** 1–5
[31] Parlinski K, Li Z and Kawazoe Y 1997 *Phys. Rev. Lett.* **78** 4063
[32] Togo A, Oba F and Tanaka I 2008 *Phys. Rev.* B **78** 134106
[33] Smidstrup S *et al* 2019 *J. Phys.: Condens. Matter* **32** 015901
[34] Henkelman G and Jónsson H 2000 *J. Chem. Phys.* **113** 9978–85
[35] Henkelman G, Uberuaga B P and Jónsson H 2000 *J. Chem. Phys.* **113** 9901–4
[36] Rijnsdorp J, De Lange G and Wiegers G 1979 *J. Solid State Chem.* **30** 365–73
[37] He Q, Yu B, Li Z and Zhao Y 2019 *Energy Environ. Mater.* **2** 264–79
[38] Sun Q, Dai Y, Ma Y, Jing T, Wei W and Huang B 2016 *J. Phys. Chem. Lett.* **7** 937–43
[39] Yadav N, Chakraborty B and Dhilip Kumar T 2020 *J. Phys. Chem.* C **124** 11293–300
[40] Ubaid M, Aziz A and Pujari B S 2021 *New J. Chem.* **45** 12647–54
[41] Meng B, Jing T and Xiao W Z 2022 *Mater. Chem. Phys.* **287** 126306
[42] Su J, Zhang J, Guo R, Lin Z, Liu M, Zhang J, Chang J and Hao Y 2019 *Mater. Design* **184** 108197
[43] Lee C and Gonze X 1995 *Phys. Rev.* B **51** 8610
[44] Sharma V K, Kanchana V, Gupta M K and Mittal R 2020 *J. Solid State Chem.* **290** 121541
[45] Hembram K, Jung H, Yeo B C, Pai S J, Kim S, Lee K R and Han S S 2015 *J. Phys. Chem.* C **119** 15041–6
[46] Heitjans P and Kärger J 2006 *Diffusion in Condensed Matter: Methods, Materials, Models* (Springer)
[47] Van der Ven A, Ceder G, Asta M and Tepesch P 2001 *Phys. Rev.* B **64** 184307
[48] Tang A, He X, Yin H, Li Y, Zhang Y, Huang S and Truhlar D G 2021 *J. Phys. Chem.* C **125** 9679–87
[49] Mortazavi M, Wang C, Deng J, Shenoy V B and Medhekar N V 2014 *J. Power Sour.* **268** 279–86
[50] Luong H D, Pham T D, Morikawa Y, Shibutani Y and Dinh V A 2018 *Phys. Chem. Chem. Phys.* **20** 23625–34
[51] Jiang H, Shyy W, Liu M, Wei L, Wu M and Zhao T 2017 *J. Mater. Chem.* A **5** 672–9
[52] Meng Y S and Arroyo-de Dompablo M E 2009 *Energy Environ. Sci.* **2** 589–609
[53] Zhu J, Alshareef H N and Schwingenschlögl U 2017 *Appl. Phys. Lett.* **111** 043903
[54] Ceder G, Chiang Y M, Sadoway D, Aydinol M, Jang Y I and Huang B 1998 *Nature* **392** 694–6